

Residual stress measurement in carbon coatings of optical fibers from the fiber bending curvature and coating thickness difference

Sham-Tsong Shiue, Hung-Chien Lin, Ting-Ying Shen, and Hao Ouyang

Citation: [Applied Physics Letters](#) **86**, 251910 (2005); doi: 10.1063/1.1946912

View online: <http://dx.doi.org/10.1063/1.1946912>

View Table of Contents: <http://scitation.aip.org/content/aip/journal/apl/86/25?ver=pdfcov>

Published by the [AIP Publishing](#)

Articles you may be interested in

[Effect of temperature cycling on the static fatigue of double-coated optical fibers](#)

J. Appl. Phys. **96**, 2494 (2004); 10.1063/1.1772882

[Transient thermal loading induced microbending loss in carbon-coated optical fibers](#)

J. Appl. Phys. **88**, 6987 (2000); 10.1063/1.1323536

[Thermally induced microbending losses in double-coated optical fibers during temperature cycling](#)

J. Appl. Phys. **88**, 3840 (2000); 10.1063/1.1309033

[Thermal stresses in hermetically double-coated optical fibers](#)

J. Appl. Phys. **85**, 3044 (1999); 10.1063/1.369641

[Thermal stresses in metal-coated optical fibers](#)

J. Appl. Phys. **83**, 5719 (1998); 10.1063/1.367427

The advertisement features a red and white color scheme. On the left, text reads 'Confidently measure down to 0.01 fA and up to 10 PΩ' and 'Keysight B2980A Series Picoammeters/Electrometers'. Below this is a red button with the text 'View video demo'. In the center is a photograph of the Keysight B2980A device. On the right is the Keysight Technologies logo, which consists of a red stylized waveform and the text 'KEYSIGHT TECHNOLOGIES'.

Residual stress measurement in carbon coatings of optical fibers from the fiber bending curvature and coating thickness difference

Sham-Tsong Shiue,^{a)} Hung-Chien Lin, Ting-Ying Shen, and Hao Ouyang

Department of Materials Engineering, National Chung Hsing University, Taichung, 402 Taiwan

(Received 17 February 2005; accepted 3 May 2005; published online 16 June 2005)

The residual stress measurement in carbon coatings of optical fibers is theoretically and experimentally investigated. A simple formula used to measure the residual stresses in the thin film deposited on a cylindrical substrate with the bending curvature is proposed. During a temperature drop, the carbon-coated optical fiber is bent due to the nonuniform deposition of coating materials. The axial residual stresses in carbon coatings of optical fibers can be measured from the fiber bending curvature and coating thickness difference. Furthermore, if Young's modulus of carbon coatings is known, the thermal expansion coefficient of carbon coatings can be determined. © 2005 American Institute of Physics. [DOI: 10.1063/1.1946912]

The use of hermetic coatings on silica glass fibers can greatly improve fiber reliability by preventing the mechanical fatigue, so hermetically coated optical fibers are extensively studied.¹⁻¹³ The carbon material is considered as a hermetic optical fiber coating, and the coating speed of carbon on the glass fiber has been increased to a rate sufficient to supply low-cost fibers for commercial networks.³ Therefore, the carbon-coated optical fiber is expected to be a key technology for optical transmission lines.^{1-4,6,12,13} In the real operation, thermal load is often applied on the optical fiber. Once the thermally induced residual stresses exist in the optical fiber coatings, the hermetically carbon-coated optical fibers may induce the additional bending losses or lose the hermetic properties.^{6,12} Hence, it is important to investigate the residual stress measurement in the optical fiber coatings. Recently, the residual stress measurement in thin carbon films deposited on the fused quartz rods has been examined by Raman spectroscopy and nanoindentation.¹⁴ On the other hand, the residual stress measurement in the thin film deposited on a planar substrate is extensively studied. For example, the Stoney equation is mostly used to measure these residual stresses from the bending curvature of the planar substrate.¹⁵⁻¹⁸ However, no work was found to study the residual stress measurement in a thin film deposited on a cylindrical substrate with the bending curvature. This is the motive for this work to theoretically and experimentally investigate the residual stress measurement in carbon coatings of optical fibers.

Figure 1 shows that a carbon-coated optical fiber is constructed of a glass fiber coated by a carbon material. Here, the Cartesian coordinate (X, Y, Z) is adopted. The cross section of the glass fiber is a solid circle with its center at the origin and its radius being r_0 . Alternatively, the carbon coatings are not uniformly deposited on the glass fiber surface. The maximum and minimum thicknesses of the carbon coating are t_2 and t_1 , respectively. The inner surface of the carbon coating coincides with the outer surface of the glass fiber, and the outer surface of the carbon coating cross section is a circle with its center at $[0, -(t_2 - t_1)/2]$. The symbols E and α represent Young's modulus and the thermal expansion coefficient, respectively, and the subscripts "0" and "1" indicate

the glass fiber and carbon coating, respectively. The thermal expansion coefficient of materials is defined as the average value of the thermal expansion coefficients during the initial and final temperatures.

Because the thermal expansion coefficients of the glass fiber and carbon coating differ, thermal stresses will build up after the temperature drop ΔT . Based on the derivations in Ref. 6, when the glass fiber and carbon coating are assumed to be elastic, the thermally induced axial force can be obtained as $F_z(C) = -F_z(G) = (\alpha_1 - \alpha_0)\Delta T E_0 E_1 A_0 A_1 / (E_0 A_0 + E_1 A_1)$. Here, $F_z(G)$ and $F_z(C)$ indicate the thermally induced axial forces in the glass fiber and carbon coating, respectively. Although $F_z(G)$ and $F_z(C)$ have the same magnitude, $F_z(G)$ is a compressive force and $F_z(C)$ is a tensile force. $A_0 (= \pi r_0^2)$ and $A_1 [= \pi(t_2 + t_1)r_0]$ represent the cross-sectional areas of the glass fiber and carbon coating, respectively. Because $E_0 A_0$ greatly exceeds $E_1 A_1$, $(E_0 A_0 + E_1 A_1)$ can be reduced to $E_0 A_0$. The centroids of $F_z(G)$ and $F_z(C)$ are located at $(0, 0)$ and $[0, -A_0(t_2 - t_1)/2A_1]$, respectively. Hence, the thermally induced axial forces $F_z(G)$ and $F_z(C)$ would produce a bending moment M on the YZ plane, and this bending moment M is equal to $F_z(C)A_0(t_2 - t_1)/2A_1$. The bending moment M would bend the fiber with a bending radius R . According to mechanics of materials,¹⁹ the bending radius R is equal to $(E_0 I_0 + E_1 I_1)/M$, where $I_0 (= \pi r_0^4/4)$ and $I_1 [= \pi(t_2 + t_1)r_0^3/4]$ are the moment of inertia of the glass fiber and carbon coating, respectively. Because $E_0 I_0$ greatly exceeds $E_1 I_1$, $(E_0 I_0 + E_1 I_1)$ can be reduced to $E_0 I_0$. After the

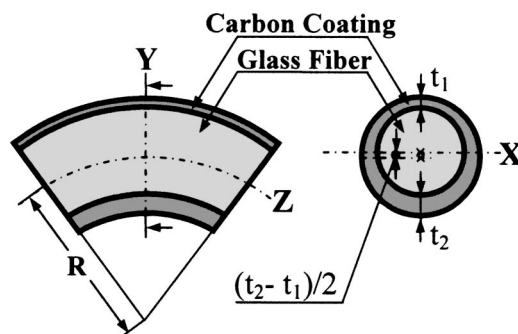


FIG. 1. Schematic diagram of a carbon-coated optical fiber with a bending radius R .

^{a)}Electronic mail: stshiue@dragon.nchu.edu.tw

rearrangement, the bending curvature $1/R$ can be represented as

$$1/R = [2(\alpha_1 - \alpha_0)\Delta TE_1(t_2 - t_1)]/(E_0 r_0^2). \quad (1)$$

Notably, Eq. (1) shows that if the carbon coating is uniformly deposited on the glass fiber surface ($t_2=t_1$), the fiber would not be bent after the temperature change.

The axial residual stress in the carbon coating is induced simultaneously by the bending moment and axial force. However, the axial force-induced axial stress is much larger than the bending moment-induced axial stress, so the axial stress in the carbon coating can be simply expressed as

$$\sigma_z = F_z(G)/A_1 = [(\alpha_1 - \alpha_0)\Delta TE_1]. \quad (2)$$

Substituting Eq. (1) into (2), Eq. (2) becomes

$$\sigma_z = (1/R)(E_0 r_0^2)/[2(t_2 - t_1)]. \quad (3)$$

For commercial optical fibers, E_0 and r_0 usually are 72.5 GPa and 62.5 μm , respectively.⁶ Consequently, if the relation between $(1/R)$ and (t_2-t_1) is known, the axial residual stress σ_z can be obtained. Notably, in order to account for the actual biaxial stress distributions in the carbon coating, rather than the uniaxial stresses assumed for ease of derivation in this work, it is necessary to replace E_0 by $E_0/(1-\nu_0)$ in Eq. (3). However, $\nu_0(=0.17)$ is small and the fiber axial length is much larger than the fiber radius, so it is not necessary to consider the effect of Poisson's ratio ν_0 in this case. Equation (3) is simple and easy to use, it is very similar to the Stoney equation used to measure the residual stress in the thin film deposited on a planar substrate from the bending curvature of the planar substrate.¹⁵⁻¹⁸

The experiment proceeded as follows. First, the carbon materials were deposited on the outer surface of the glass fiber using the plasma enhanced chemical vapor deposition (PECVD) method. The glass fiber is a standard single-mode fiber with outer diameter $2r_0$ equaling 125 μm . The carbon coating was prepared using methane during the PECVD process. Five samples of carbon-coated optical fibers with identical fiber length (≈ 100 mm) but different coating thicknesses were obtained by controlling the deposition time, with the deposition time being 10, 20, 30, 40, and 50 min, respectively. The temperature of the fiber holder was controlled at 250 $^\circ\text{C}$. After the deposition process was finished, the samples were cooled down to the room temperature (25 $^\circ\text{C}$) in the process chamber. In this step, the temperature change ΔT was 225 $^\circ\text{C}$. This experiment showed that the fibers were bent after the coating process and temperature drop were finished. The bending radius of the fiber was immediately measured by drawing the bending curve of the fiber on the graph paper. Second, the thickness of the carbon coating was obtained by measuring the cross section of the optical fiber using the scanning electron microscope (SEM). Meanwhile, Young's modulus of the carbon coating was measured using the nano-indenter (NI). Each datum of Young's modulus was obtained from the average value of ten times of indentation on the same sample. Finally, these five samples were immersed in the liquid nitrogen (77 K) for an hour. After these fiber samples were taken out of the liquid nitrogen, the bending radius of the fiber was immediately measured again. In this step, the temperature change ΔT was 446 $^\circ\text{C}$.

After the examination of SEM and NI, the thickness and Young's modulus of the carbon coating are obtained, respec-

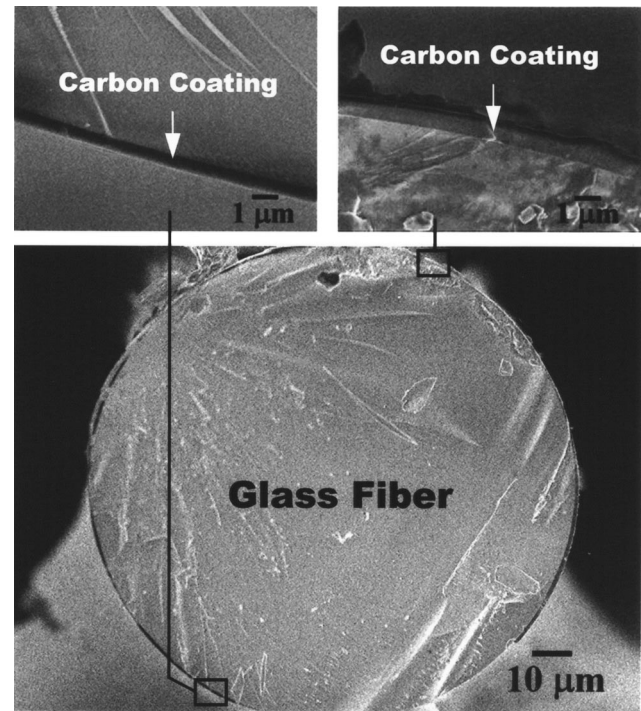


FIG. 2. An example of SEM photograph to demonstrate the cross section of the carbon-coated optical fiber, where the deposition time is 50 min.

tively. An example of an SEM photograph to demonstrate the cross section of the optical fiber is shown in Fig. 2. This figure depicts that the carbon coating is not uniformly deposited on the glass fiber surface. The fiber thicknesses (t_2 and t_1) with different deposition time are listed in Table I. Table I depicts that the coating thickness difference (t_2-t_1) is proportional to the deposition time. Meanwhile, NI examination indicates that Young's modulus of the carbon coating is about 108 GPa, in which the variation of Young's modulus with the coating thickness is very small and it is negligible. Notably, when the coating thickness is smaller than 300 nm, NI examination is not valuable due to the substrate effect. However, when the coating thickness is larger than 300 nm, the variation of Young's modulus with the coating thickness is very small. As a result, it is believed that the variation of Young's modulus with the coating thickness is negligible. Alternatively, because the ratio of fiber radius and coating thickness is not less than 84 ($=62.5 \mu\text{m}/744 \text{ nm}$), NI examination shows that the difference of Young's modulus between the carbon coating deposited on the planar substrate and cylindrical substrate is also small. The fiber bending radius with different deposition time and temperature change is also shown in Table I. Table I reveals that the bending radius

TABLE I. The carbon coating thickness and fiber bending radius at different deposition time.

| Deposition time (min) | t_2 (nm) | t_1 (nm) | t_2-t_1 (nm) | $R(\Delta T=225 \text{ }^\circ\text{C})$ (m) | $R(\Delta T=446 \text{ }^\circ\text{C})$ (m) |
|-----------------------|------------|------------|----------------|--|--|
| 10 | 149 | 105 | 44 | 78.21 | 39.46 |
| 20 | 298 | 210 | 88 | 39.11 | 19.73 |
| 30 | 447 | 315 | 132 | 26.07 | 13.15 |
| 40 | 596 | 421 | 175 | 19.66 | 9.92 |
| 50 | 744 | 527 | 217 | 15.86 | 8.00 |

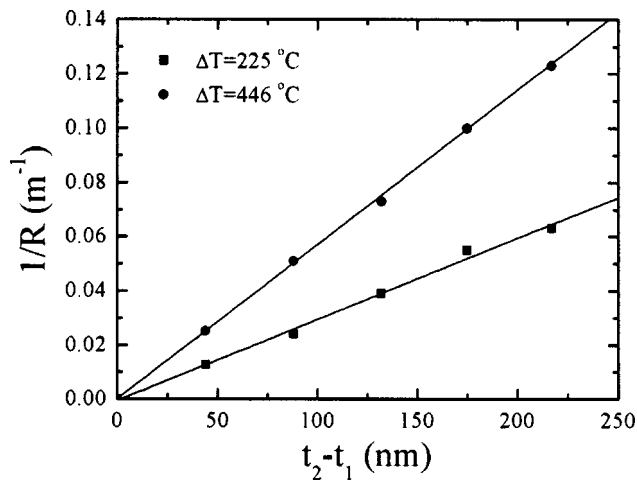


FIG. 3. The relation between the fiber bending curvature $1/R$ and coating thickness difference ($t_2 - t_1$).

is inversely proportional to the deposition time (or coating thickness difference, $t_2 - t_1$).

Figure 3 displays the fiber bending curvature $1/R$ versus ($t_2 - t_1$) at two different temperatures. This figure shows that the bending curvature $1/R$ is proportional to ($t_2 - t_1$), and it is in good agreement with the theoretical result as shown in Eq. (1). The slopes of two straight lines shown in Fig. 3 for $\Delta T = 225^\circ$ and $446^\circ C$ are 3×10^5 and $5.7 \times 10^5 m^{-2}$, respectively. Equation (3) reveals that if $r_0 = 62.5 \mu m$ and $E_0 = 72.5 GPa$, the axial residual stresses in the carbon coating for $\Delta T = 225^\circ$ and $446^\circ C$ are 42.5 and 80.7 MPa, respectively. Furthermore, Eq. (1) shows that the line slope in Fig. 3 is equal to $[2(\alpha_1 - \alpha_0)\Delta TE_1]/(E_0 r_0^2)$. As a result, if $r_0 = 62.5 \mu m$, $E_0 = 72.5 GPa$, $E_1 = 108 GPa$, and $\alpha_0 = 0.56 \times 10^{-6}/^\circ C$,⁶ one obtains that α_1 is equal to 2.31×10^{-6} and $2.24 \times 10^{-6}/^\circ C$ for $\Delta T = 225^\circ$ and $446^\circ C$, respectively. The value of α_1 in this study is in good agreement with that reported in the literature.²⁰

It is worthy to mention that, if Young's modulus is determined by the NI method, the measured Young's modulus is not the exact Young's modulus of the coating materials. Usually, the measured Young's modulus E_r can be expressed as $1/E_r = [(1 - \nu_s^2)/E_s] + [(1 - \nu_i^2)/E_i]$, where E_s and E_i are Young's modulus of the sample and indenter, respectively, and ν_s and ν_i are Poisson's ratios of the sample and indenter, respectively. However, it is not necessary to know ν_s with

great precision because Young's modulus is influenced insignificantly by ν_s in the evaluation of E_r .²¹ Therefore, the effect of Poisson's ratio on the measured Young's modulus is not considered here.

In summary, a simple equation used to measure the residual stresses in the thin film deposited on a cylindrical substrate with the bending curvature is proposed. The axial residual stress in carbon coatings of optical fibers can be measured from the relation between the fiber bending curvature and coating thickness difference. Furthermore, if Young's modulus of the carbon coating is known, the thermal expansion coefficient of the carbon coating can be determined.

This work was supported by the National Science Council, Taiwan, Republic of China, under Grant No. NSC 93-2215-005-003.

¹K. E. Lu, G. S. Glaesemann, R. V. VanDewoestine, and G. Kar, *J. Lightwave Technol.* **6**, 240 (1988).

²N. Yoshizawa and Y. Katsuyama, *Electron. Lett.* **25**, 1429 (1989).

³N. Yoshizawa, H. Tada, and Y. Katsuyama, *J. Lightwave Technol.* **9**, 417 (1991).

⁴A. H. Lettington and C. Smith, *Diamond Relat. Mater.* **1**, 805 (1992).

⁵D. R. Biswas, *Opt. Eng.* **31**, 1400 (1992).

⁶S. T. Shiue and W. H. Lee, *J. Mater. Res.* **12**, 2493 (1997).

⁷S. T. Shiue and Y. S. Lin, *J. Appl. Phys.* **83**, 5719 (1998).

⁸H. S. Seo, U. C. Paek, K. Oh, and C. R. Kurkjian, *J. Lightwave Technol.* **16**, 2355 (1998).

⁹S. T. Shiue, *J. Appl. Phys.* **85**, 3044 (1999).

¹⁰S. T. Shiue, P. T. Lien, and J. L. He, *J. Appl. Phys.* **87**, 3759 (2000).

¹¹S. T. Shiue, L. Y. Pan, and H. H. Hsiao, *Mater. Chem. Phys.* **78**, 518 (2002).

¹²S. T. Shiue, J. L. He, L. Y. Pan, and S. T. Huang, *Thin Solid Films* **406**, 210 (2002).

¹³K. H. Kwok and W. K. S. Chiu, *Carbon* **41**, 673 (2003).

¹⁴C. A. Taylor, M. F. Wayne, and W. K. S. Chiu, *Thin Solid Films* **429**, 190 (2003).

¹⁵Z. Sun, C. H. Lin, Y. L. Lee, J. R. Shi, B. K. Tay, and X. Shi, *Thin Solid Films* **377-378**, 198 (2000).

¹⁶E. Tomasella, L. Thomas, C. Meunier, M. Nadal, and S. Mikhailov, *Surf. Coat. Technol.* **174-175**, 360 (2003).

¹⁷G. Capote, F. L. Freire, L. G. Jacobsohn, and G. Mariotto, *Diamond Relat. Mater.* **13**, 1454 (2004).

¹⁸M. Lejeune, M. Benlahsen, and R. Bouzerar, *Appl. Phys. Lett.* **84**, 344 (2004).

¹⁹J. M. Gere, *Mechanics of Materials*, 5th ed. (Brooks/Cole, a division of Thomson Learning, Pacific Grove, CA, 2001).

²⁰A. Champi, R. G. Lacerda, and F. C. Marques, *Thin Solid Films* **420-421**, 200 (2002).

²¹X. Jiang, K. Reichelt, and B. Stritzker, *J. Appl. Phys.* **66**, 5805 (1989).